

Forced Imbibition to Enhanced Tight/Shale Oil Recovery: A Molecular Dynamics Simulation Study

Wang Shun^{1,2}, Wang Jing^{1,2*}, Liu Huiqing^{1,2}

(1. State Key Laboratory of Petroleum Resources and Prospecting in China University of Petroleum, Beijing 102249, China; 2. MOE Key Laboratory of Petroleum Engineering in China University of Petroleum, Beijing 102249, China)

ABSTRACT

Huff-puff by water has been conducted to enhance oil recovery after hydraulic fracturing in tight/shale oil reservoirs. However, the microscopic mechanism behind this approach is still unclear, which significantly limits the efficient development of tight oil. In order to reveal the oil and water transport law in nano scale during huff-puff by water, the whole process of pressurizing, high-pressure soaking, and depressurizing was studied by molecular simulation technology. The micro mechanism of crude oil transport at each stage was analyzed, and the effects of reservoir temperature, soaking pressure and soaking time on the transport characteristics of crude oil are investigated. The results show that the crude oil in the pore moves along the positive direction of pressure gradient, and the velocity increases first and then decreases in the pressurizing stage. In the soaking stage, the boundary layer oil molecules move along the positive direction of pressure gradient, while the bulk oil moves along the negative direction of pressure gradient under imbibition. In the depressurizing stage, the crude oil velocity increases rapidly first and then gradually flattens; The same direction of huff and puff system (TSDS) is more beneficial to improve tight oil forced imbibition recovery than the opposite direction of huff and puff system (TODS), and the recovery of TSDS is about 4 times that of TODS; Increasing temperature has a significant effect on each stage of forced imbibition, and the recovery increases about 2% for every 20°C increase in temperature. The pressure increase only has a significant effect on the depressurizing process. For every 10MPa increase in pressure, the recovery increases by 2%; Prolonged soaking time can significantly improve the recovery in the opposite direction of huff and puff system. This work further reveals the micro mechanism

of fluid transport in nano-pores during the high-pressure soaking and drainage process of tight oil, providing theoretical guidance for efficiently adjusting the pressurizing, soaking, and depressurizing system to improve tight oil recovery.

Keywords: Tight/shale oil; Forced Imbibition; Huff-puff; Molecular Simulation; Transportation

1. INTRODUCTION

There is significant oil content in unconventional shale resources that cannot be recovered using primary depletion stage because of small pore sizes and extremely low permeability of shale matrix^[1]. Therefore, spontaneous imbibition under capillary force is considered to be the main mechanism of tight oil development after reservoir fracturing, and a large number of studies have shown that spontaneous imbibition can effectively improve tight core recovery^[2-4]. However, the actual reservoir is under pressure, which is not ideal spontaneous imbibition. There are significant differences between forced imbibition and spontaneous imbibition^[5, 6]. For example, Wang, et al^[7] established a mechanistic mode for forced imbibition, they demonstrated that high-pressure soaking plays an essential role in oil production by both imbibition and elasticity after hydraulic fracturing. In addition, different depressurized production methods lead to different fluid transport mechanisms, so it is necessary to clarify the microscopic fluid transport mechanism in the process of forced imbibition and depressurized drainage in tight pores, so as to provide guidance for efficient development of tight oil.

With the rapid development of computer technology, molecular simulation has been widely used to study fluid transport mechanisms in nanopores. Since

molecular simulation allows complete control of components and simulation conditions in the model and provides a detailed and intuitive atomic-scale simulation process, greatly facilitating the interpretation of experimental results at the microscopic level, these advantages have aroused widespread interest among researchers^[8-13]. Wang et al^[14]. studied the effect of polar molecules on spontaneous imbibition in nano pores by molecular simulation, and they proved that the adsorption energy and orientation Angle of polar molecules are the key factors affecting imbibition. Stukan, et al^[15]. present Molecular Dynamics simulations of the imbibition process in nanopores in case of two different mechanisms of the wettability modification, and they find that qualitative difference in the imbibition dynamics in the two cases and indicate that MD simulation is a useful tool to investigate details of the imbibition mechanisms at the pore scale with direct implications for Enhanced Oil Recovery (EOR) operations.

In view of the above problems, this paper studies the fluid transport law in the whole process of forced imbibition and depressurizing in nano-pores by using molecular simulation method, and analyzes the influence of reservoir temperature, pressure, soaking time and drainage mode on the transport mechanism. Our research is of great significance for the efficient development of tight oil and the solution to the current energy crisis.

2. METHODOLOGY

2.1 Model construction

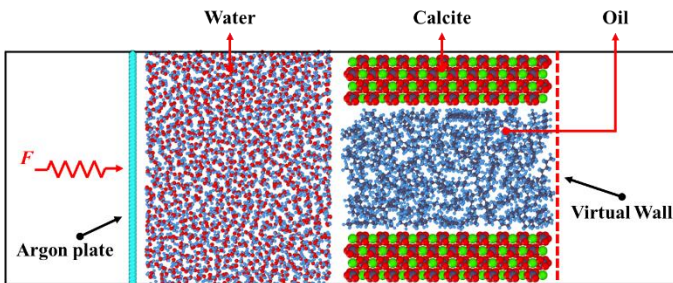


Fig. 1 Initial configuration

The construction process of the three-dimensional periodic molecular model is as follows: (1) The calcite crystal was derived from the Materials Studio software model library and cut along the (1 0 4) surface. Then, the crystal was extended to the calcite wall surface of 1.70 nm×5.00 nm×1.07 nm. (2) Construct a crude oil model containing 100 octane molecules. (3) Construct a water box model containing 1500 water molecules. (4) Splice

the calcite, crude oil layer and water box by using the build layer command, as shown in Fig. 1. (5) Finally, an argon plate is added to the left side of the water box for the pressurization process, and 3nm vacuum layers were added on both sides of the box to avoid the influence of periodic boundary conditions.

2.2 Potential models

The accuracy of molecular dynamics rests on the correct choice of mathematical equations and interaction parameters for the potential energy. In this study, water molecules were described by the TIP4P model^[16]. In order to be consistent with the convention used in the development of this force field, the OPLS-AA model of the all-atomic force field is adopted to characterize alkane molecules^[17]. The general form of its mathematical model is as follows:

$$E = E_{\text{bonds}} + E_{\text{angle}} + E_{\text{dihedrals}} + E_{\text{nonbonded}} \quad (1)$$

$$E_{\text{bonds}} = \sum_{\text{bonds}} K_r (r - r_0)^2 \quad (2)$$

$$E_{\text{angles}} = \sum_{\text{angles}} K_\theta (\theta - \theta_0)^2 \quad (3)$$

$$E_{\text{dihedrals}} = \frac{C_1}{2} [1 + \cos(\alpha - \alpha_0)] + \frac{C_2}{2} [1 - \cos 2(\alpha - \alpha_0)] + \quad (4)$$

$$\frac{C_3}{2} [1 + \cos 3(\alpha - \alpha_0)] + \frac{C_4}{2} [1 - \cos 4(\alpha - \alpha_0)]$$

$$E_{\text{nonbonded}} = \sum_{i>j} \left\{ 4\epsilon_{ij} f_{ij} \left[\left(\frac{\sigma_{ij}}{r_{ij}} \right)^{12} - \left(\frac{\sigma_{ij}}{r_{ij}} \right)^6 \right] + \frac{q_i q_j e^2}{r_{ij}} \right\}, r < r_{\text{cut}} \quad (5)$$

2.3 Simulation details

The Large-scale Atomic/Molecular Massively Parallel Simulator (LAMMPS), distributed by Sandia National Laboratories, was utilized to perform MD simulations^[18]. First, the potential energy of the initial configuration (Fig.1) was minimized by iterative adjustment of these atomic coordinates using the conjugate gradient algorithm with the calcite and Ar plate in the initial configuration fixed. The system was then relaxed for 500 ps under NVT ensemble, and the temperature of the system is controlled by Berendsen algorithm at 333K. After that, Then apply different pressure to the argon plate to simulate the process of pressurizing the well. Finally, open different end faces to simulate the process of depressurizing. The Nosé-Hoover algorithm was used to control the system's temperature (coupling constant: 0.1ps), and data were collected at 1ps intervals for statistical analysis^[19]. The visualization results in this paper are realized by Ovito Basic 3.4.4 software^[20].

3. RESULTS

By analyzing the density distribution of oil phase and the change of oil phase centroid velocity in the process of pressure imbibition, the transport law of oil phase was characterized, and the internal mechanism of the transport law was further revealed by analyzing the energy of oil phase.

3.1 Molecular simulation results

Fig. 2 shows the two-dimensional density distribution of oil in the pores at the high-pressure soaking stage. It can be seen from the Fig. 2 that the density of oil phase near the boundary layer is significantly higher than that of bulk phase, which is caused by the strong interaction between the pore wall and the crude oil molecules. It is also found that the density of the oil phase at the end of the pore is higher than that at the entrance of the pore.

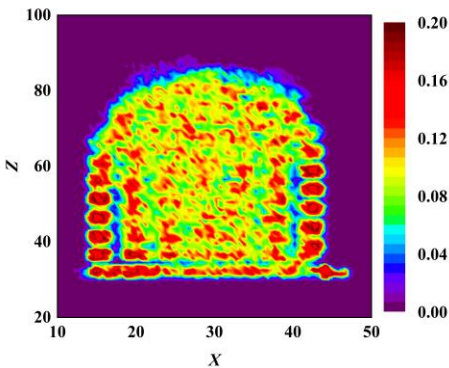


Fig. 2 Oil density in the soaking stage

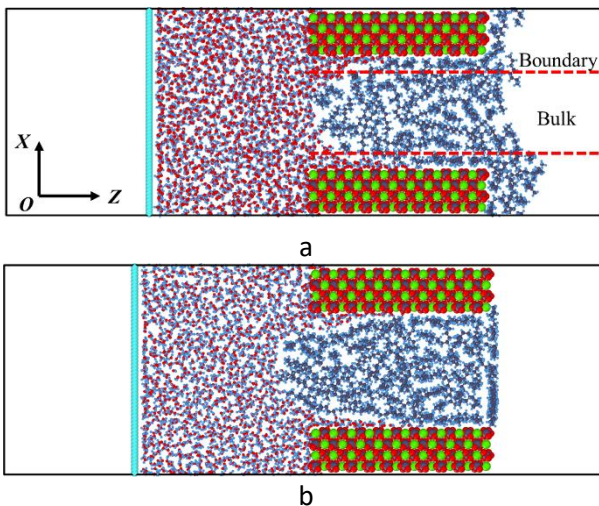


Fig. 3 The final configurations a: TSDS; b: TODS

Fig. 3a, b are the final configuration diagrams of the system with the same direction of huff and puff (Hereinafter referred to as TSDS) and the system in the opposite direction of huff and puff (Hereinafter referred

to as TODS) respectively. It can be seen intuitively that the recovery of the same direction system is higher than that of the opposite direction system under the same conditions.

3.1.1 Transportation law

The center of mass (COM) velocity changes of crude oil boundary and bulk over time in the same direction system and the opposite direction system were monitored, as shown in Fig. 4.

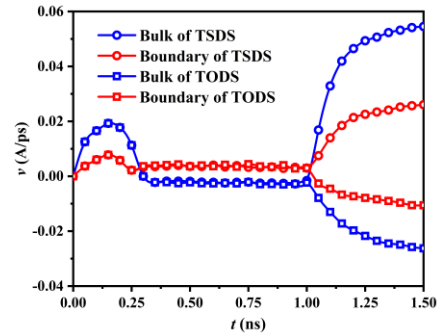


Fig. 4 The center of mass velocity of the crude oil varies with time

In this paper, TSDS and TODS are only different in the depressurizing stage, the boundary and bulk phase of the two methods have the same velocity change rule in the pressurization and the soaking stage. In the pressurization stage, the fluid accelerates under the action of external forces, and the intermolecular repulsion gradually increases as the volume is compressed. When the molecular repulsion force balances with the external force, the velocity reaches the maximum value. Further compression of the volume leads to a further increase in intermolecular repulsion, resulting in a gradual decrease of the velocity to 0. The argon plate is fixed at the high-pressure soaking stage, and boundary water molecules invade deep pores under the interaction with the wall and drive boundary layer oil molecules to deep pores, while bulk oil molecules move along the negative direction of Z axis. When entering the depressurizing stage, the crude oil molecules in the TSDS are discharged from the pores along the Z-axis in the positive direction, but in the negative direction at a relatively small speed in TODS. In both cases, the velocity of the boundary layer is less than the bulk phase velocity.

3.1.2 Interaction mechanism

We calculated the interaction between crude oil molecules in the whole time domain to reveal the internal mechanism of the above transport law, as shown in Fig. 5. It shows that the increase of crude oil energy at the pressurized results in the enhancement of

intermolecular repulsion. When entering the soaking stage, the crude oil energy keep constant, and oil molecules in high energy condition. Once enters the depressurizing stage, the high-energy state of the system is released. The energy decline of TSDS is much greater than that of TODS, and the reduced energy is converted into the kinetic energy of oil molecules, so the speed of TSDS is greater than that of TODS.

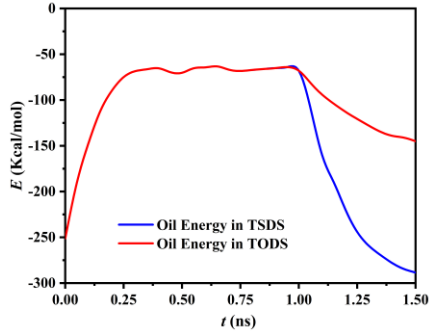


Fig. 5 The energy of oil droplets varies with time

3.1.3 Recovery

In order to quantitatively compare the recovery of TSDS and TODS under the same conditions, we monitored the number of carbon atoms in the alkane molecules at the outlet end of the outflow pores at different times, and the change of recovery over time as shown in Fig. 6.

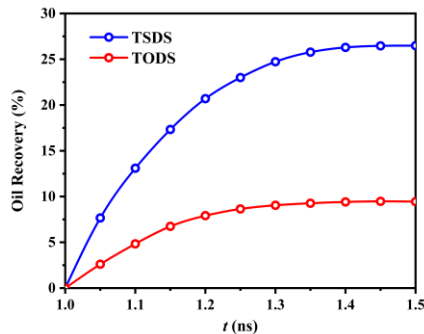


Fig. 6 Change in recovery over time

It can be seen that the oil recovery of TSDS is about 26.4%, which is about 4 times that of TODS.

3.2 Effects of temperature

We studied the changes of bulk and boundary velocity over time in TSDS at 40°C, 60°C and 80°C to study the influence of reservoir temperature on forced imbibition as shown in Fig. 7.

As can be seen, the velocity of the bulk phase decreases with the increase of temperature in the pressurizing process; the velocity of the bulk phase fluid along the negative direction of Z axis increases with the

increase of temperature in the soaking stage; and the velocity of the bulk phase fluid increases with the increase of temperature in the depressurizing stage. The velocity of boundary layer molecules and bulk changes with temperature in a similar way, but the difference lies in the positive z-axis movement of boundary layer fluid driven by water molecules in the soaking stage. This is because the molecular thermal motion intensifies with the increase of temperature, and the intense molecular collision makes it difficult to compress in the pressurizing stage. The high temperature in the soaking and depressurizing stage will aggravate the molecular motion, resulting in the increase of velocity.

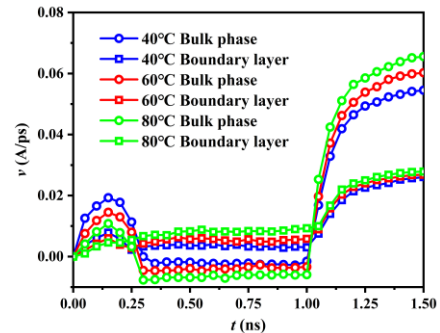


Fig. 7 The change in velocity at different temperatures

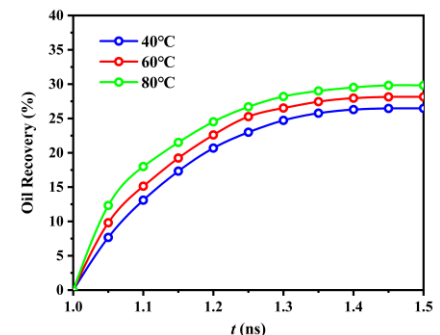


Fig. 8 Recovery at different temperatures

In addition, the recovery change over time at different temperatures was calculated, as shown in Fig. 8. It can be seen that the recovery is positively correlated with temperature under the same conditions. For every 20°C increase in temperature, recovery increases by about 2 percentage points.

3.3 Effects of press

Similarly, we studied the changes of bulk and boundary velocity over time in TSDS at 30MPa, 70MPa and 90MPa to study the influence of reservoir pressure on forced imbibition, as shown in Fig. 9.

It can be seen from Fig. 9 that the velocity of bulk phase and boundary layer increases slightly with the increase of pressure in the process of pressurizing and

soaking, this is due to the increase of pressure on the one hand can accelerate the movement of molecules along the pressure gradient; on the other hand, under the action of large pressure, the space between molecules is compressed and the movement of molecules is blocked. The synergistic effect of these two effects results in poor sensitivity of the motion velocity to pressure in these two stages. However, in the depressurizing stage, the larger intermolecular repulsive force makes the velocity increase significantly with the increase of pressure.

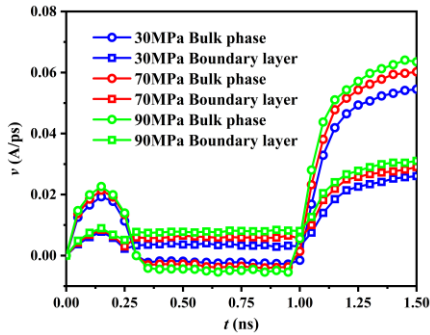


Fig. 9 The change in velocity at different pressures

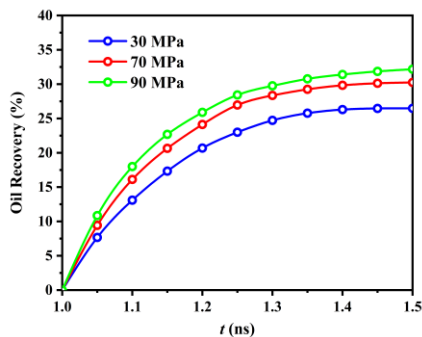


Fig. 10 Recovery at different pressures

In addition, the recovery change over time at different pressures was calculated, as shown in Fig. 10. It can be seen that the recovery is positively correlated with temperature under the same conditions. The recovery also increases by about 2 percentage points for every 10MPa increase in pressure.

3.4 Effects of soaking time

In order to explore the influence of soaking time on pressurized imbibition in nano-pores, we calculated TSDS and TODS recovery under different soaking time respectively, as shown in Fig. 11.

As can be seen from the Fig. 11, the contribution of prolonged soaking time to recovery is not significant for TSDS, while the contribution of extended soaking time to recovery is significantly increased for TODS. This is because in the soaking stage, the bulk phase moves toward the negative direction of Z axis, and the bulk

phase crude oil occupies a large proportion in the pores. Therefore, when the soaking time is prolonged, more bulk phase molecules will move to the outlet section, resulting in more oil molecules being recovered in the depressurizing stage. However, for TSDS, prolonging the soaking time will increase the movement of boundary layer oil molecules towards the outlet, but the number of boundary layer molecules is small, so the enhanced oil recovery effect is not obvious.

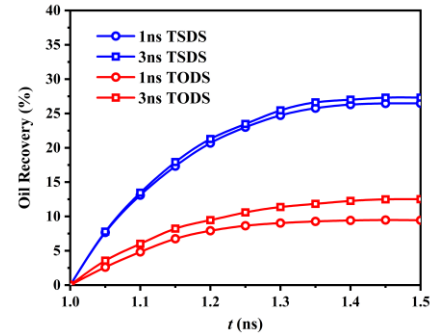


Fig. 11 Recovery at different soaking times

4. CONCLUSIONS

1. During the pressurizing stage, the fluid moves in the positive direction of the pressure gradient, and the moving speed increases first and then decreases to 0. In the soaking stage, bulk fluid moves along the negative direction of pressure gradient, while boundary fluid moves along the positive direction of pressure gradient. In the depressurization stage, the velocity of fluid firstly increases rapidly and then gradually flattens.

2. The recovery of TSDS is higher than that of TODS under the same conditions

3. The temperature change has significant influence on the fluid movement in the whole process of forced imbibition, while the pressure change has significant influence on the depressurizing stage, but has little influence on the pressurizing and soaking stage.

4. Prolonged soaking time can significantly improve recovery of TODS.

ACKNOWLEDGEMENT

This work was supported by the National Natural Science Foundation of China (No. 52074316) and the Science Foundation of China University of Petroleum, Beijing (No. 2462018QNXZ01). The authors would like to sincerely acknowledge these funds for their financial support.

REFERENCE

- [1] Takbiri-Borujeni A, Kazemi M, Liu S, et al. Molecular Simulation of Enhanced Oil Recovery in Shale[J]. *Energy Procedia*. 2019, 158: 6067-6072.
- [2] Wang C, Gao H, Gao Y, et al. Influence of Pressure on Spontaneous Imbibition in Tight Sandstone Reservoirs[J]. *Energy & Fuels*. 2020, 34(8): 9275-9282.
- [3] Dou L, Xiao Y, Gao H, et al. The study of enhanced displacement efficiency in tight sandstone from the combination of spontaneous and dynamic imbibition[J]. *Journal of Petroleum Science and Engineering*. 2021, 199: 108327.
- [4] Cai J, Li C, Song K, et al. The influence of salinity and mineral components on spontaneous imbibition in tight sandstone[J]. *Fuel*. 2020, 269: 117087.
- [5] Sharma J, Inwood SB, Kavscek A. Experiments and analysis of multiscale viscous fingering during forced imbibition[J]. *SPE J.*, 2012, 17(4): 1142-1159.
- [6] Meng Qingbang, Cai Jianchao, Wang Jing. Scaling of countercurrent imbibition in 2D matrix blocks with different boundary conditions[J]. *SPE J.*, 2019, 24(3): 1179-1191.
- [7] Jing W, Huiqing L, Genbao Q, et al. Investigations on spontaneous imbibition and the influencing factors in tight oil reservoirs[J]. *Fuel*. 2019, 236: 755-768.
- [8] Lu G, Zhang X, Shao C, et al. Molecular dynamics simulation of adsorption of an oil-water-surfactant mixture on calcite surface[J]. *Petroleum Science*. 2009, 6(1): 76-81.
- [9] Koleini MM, Badizad MH, Kargozarfard Z, et al. The impact of salinity on ionic characteristics of thin brine film wetting carbonate minerals: An atomistic insight[J]. *Colloids and Surfaces A: Physicochemical and Engineering Aspects*. 2019, 571: 27-35.
- [10] Koleini MM, Badizad MH, Hartkamp R, et al. The Impact of Salinity on the Interfacial Structuring of an Aromatic Acid at the Calcite/Brine Interface: An Atomistic View on Low Salinity Effect[J]. *J Phys Chem B*. 2020, 124(1): 224-233.
- [11] Santos Silva H, Alfarra A, Vallverdu G, et al. Asphaltene aggregation studied by molecular dynamics simulations: role of the molecular architecture and solvents on the supramolecular or colloidal behavior[J]. *Petroleum Science*. 2019, 16(3): 669-684.
- [12] Kirch A, Mutisya SM, Sánchez VM, et al. Fresh Molecular Look at Calcite-Brine Nanoconfined Interfaces[J]. *The Journal of Physical Chemistry C*. 2018, 122(11): 6117-6127.
- [13] Dimitrov DI, Milchev A, Binder K. Forced imbibition- a tool for separate determination of Laplace pressure and drag force in capillary filling experiments[J]. *Phys. Chem. Chem. Phys.*, 2008, 10: 1867-1869.
- [14] Wang S, Wang J, Liu H, et al. Impacts of Polar Molecules of Crude Oil on Spontaneous Imbibition in Calcite Nanoslit: A Molecular Dynamics Simulation Study[J]. *Energy & Fuels*. 2021, 35(17): 13671-13686.
- [15] M.R. Stukan, P. Ligneul, E.S. Boek. Molecular Dynamics Simulation of Spontaneous Imbibition in Nanopores and Recovery of Asphaltenic Crude Oils Using Surfactants for EOR Applications[J]. *Oil & Gas Science and Technology-Revue D IFP ENERGIES Nouvelles* 2012; 67(5):737-742.
- [16] Abascal J L F, Sanz E, García Fernández R, et al. A potential model for the study of ices and amorphous water: TIP4P/Ice[J]. *The Journal of Chemical Physics* 2005; 122(23): 234511.
- [17] Jorgensen W L, Maxwell D S, Tirado-Rives J. Development and testing of the OPLS all-atom force field on conformational energetics and properties of organic liquids[J]. *Journal of the American Chemical Society* 1996; 118(45): 11225-11236.
- [18] Plimpton S. Fast parallel algorithms for short-range molecular dynamics[J]. *Journal of Computational Physics* 1995; 117(1): 1-19.
- [19] Sen W. *Microscale Flow Mechanisms of Oil in Shale*[D]. China University of Petroleum, 2016.
- [20] Stukowski A. Visualization and analysis of atomistic simulation data with OVITO-the Open Visualization[J]. *Tool Modelling Simul Mater Sci Eng* 2010; 18: 015012.